



Heterobimetallic tin(II) oxido clusters of the type $\{\text{Sn}_6(\mu_3\text{-O})_4(\mu_3\text{-OCH}_2\text{R})_4\}\{\text{W}(\text{CO})_5\}_4$ and $\{\{\text{Sn}_5(\mu_3\text{-O})_2(\mu\text{-OCH}_2\text{R})_4(\mu_3\text{-OCH}_2\text{R})_2\}\{\text{Fe}(\text{CO})_4\}_2\}$

Lutz Mertens ^a, Christian Leonhardt ^a, Tobias Rüffer ^b, Ana Toma ^c, Cristian Silvestru ^c, Michael Mehring ^{a,*}

^a Technische Universität Chemnitz, Institut für Chemie, Koordinationschemie, D-09107 Chemnitz, Germany

^b Technische Universität Chemnitz, Institut für Chemie, Anorganische Chemie, D-09107 Chemnitz, Germany

^c Departamentul de Chimie, Centrul de Chimie Supramoleculară Organica și Organometalică (CCSOOM), Facultatea de Chimie și Inginerie Chimică, Universitatea Babeș-Bolyai, 400028 Cluj-Napoca, Romania

ARTICLE INFO

Article history:

Received 4 February 2016

Received in revised form

14 April 2016

Accepted 20 April 2016

Available online xxx

Dedicated to Prof. Heinrich Lang on the occasion of his 60th birthday

Keywords:

Tin alkoxides

Tin oxido clusters

Tin-tungsten complexes

Tin-iron complexes

Hydrolysis

ABSTRACT

Reaction of the tin(II) alkoxides bis(2-methoxyphenylmethanolate)tin(II) (**1**) and bis(2,4-dimethoxyphenylmethanolate)tin(II) (**2**) with $[\text{W}(\text{CO})_5(\text{thf})]$ and $[\text{Fe}_2(\text{CO})_9]$, respectively, gave the heterobimetallic tin(II) oxido clusters $\{\{\text{Sn}_6(\mu_3\text{-O})_4(\mu_3\text{-OCH}_2\text{R})_4\}\{\text{W}(\text{CO})_5\}_4\}$ [**3**, R=C₆H₄(OCH₃)₂-2,4]; **4**, R=C₆H₃(OCH₃)₂-2,4] and $\{\{\text{Sn}_5(\mu_3\text{-O})_2(\mu\text{-OCH}_2\text{R})_4(\mu_3\text{-OCH}_2\text{R})_2\}\{\text{Fe}(\text{CO})_4\}_2\}$ [**5**, R=C₆H₃(OCH₃)₂-2,4] which were isolated reproducibly with fair yield as a result of partial hydrolysis in the presence of moisture. The metal oxido clusters are composed of polynuclear tin(II) oxido cages entrapped by arylmethanolate ligands and coordinated to metal carbonyl moieties via lone pairs of electrons at tin. The compounds were analyzed by single crystal X-ray diffraction analysis (**1**, **4**·2THF and **5**), elemental analyses, ATR-IR spectroscopy and ¹H, ¹³C{¹H} and ¹¹⁹Sn{¹H} NMR spectroscopy in solution as well as in solid state.

© 2016 Elsevier B.V. All rights reserved.

1. Introduction

Homo- and heterobimetallic tin oxides have found widespread applications as, e.g. gas sensors, solar cells, thermoelectric converters, phosphors, coatings, catalysts and anode materials for Li-ion batteries [1–6]. Production technologies for these materials in water are promising with regard to large scale, cost efficiency and environmental compatibility. However, solution-based approaches towards tin oxide based nanomaterials and coatings starting from tin salts in aqueous media are difficult to control due to the low solubility of tin oxido hydroxides, which are readily formed in aqueous solution. Tin alkoxides, which offer the advantage of high solubility

in a variety of organic solvents, present an alternative, e.g. in sol-gel chemistry for thin film formation [7,8]. In addition volatile tin alkoxides and oxido alkoxides might be used in technological processes based on chemical vapor deposition [9–11]. Because of their water sensitivity tin alkoxides are easily converted into oligomeric tin oxido alkoxido clusters, which might often be an advantage rather than a disadvantage for solution-based processes. Small clusters show increased stability, better handling and often higher solubility as compared to the parent tin alkoxides. The most prominent cluster geometry for tin oxido clusters is based on a hexanuclear octahedral arrangement of tin atoms, which was first reported for the tin(II) oxido hydroxido compound $[\text{Sn}_6(\mu_3\text{-O})_4(\mu_3\text{-OH})_4]$ in 1968. However, this tin species is of low solubility as a result of lacking solubilizing alkoxido ligands [12]. Since this study several hexanuclear tin oxido alkoxides of similar basic structure have been reported, e.g. $[\text{Sn}_6(\mu_3\text{-O})_4(\mu_3\text{-OR})_4]$ (R=Me [9,13,14], Et [9,14], iPr [14], tBu [15], neoPent [16], CH₂CH₂NMe₂, [9]). Most often these clusters are a result of partial hydrolysis, but in case of $[\text{Sn}_6(\mu_3\text{-O})_4(\mu_3\text{-OSiMe}_3)_4]$ the cluster forms as a result of silyl ether-elimination starting from

* Corresponding author. Present address: Technische Universität Chemnitz, D-09107 Chemnitz, Germany.

E-mail addresses: lutz.mertens@chemie.tu-chemnitz.de (L. Mertens), christian.leonhardt@s2005.tu-chemnitz.de (C. Leonhardt), tobias.rueffer@chemie.tu-chemnitz.de (T. Rüffer), atoma@chem.ubbcluj.ro (A. Toma), cristian.silvestru@ubbcluj.ro (C. Silvestru), michael.mehring@chemie.tu-chemnitz.de (M. Mehring).

[Sn(OSiMe₃)₂]₂ [17,18]. Other nuclearities and structures for tin(II) oxido clusters are realized for example, in [Sn₅(μ₃-O)₂(μ-OR)₄(μ₃-OR)₂] (R=neoPent) [16], and for tin(IV) in [Sn₃(μ₃-O)₂(μ-OiBu)₃(Oi-Bu)₇(Ho*i*Bu)₂] [19], [Sn₄(μ₃-O)₂(μ-OEt)₄(OEt)₆(η²-acac)₂] [20], [Sn₅(OH)₂(μ-OH)₂(μ₃-O)₂{(OC₂H₅CH₂)(OCMe₂CH₂)₂N}₄] [21], [Sn₆O₆(OAc)₆(OtBu)₆] [22], [Sn₃(μ₃-O)₂(μ-OH)₂(μ-OR)₃(OR)₆(HOR)]₂ (R=CH₂C₄H₉S) [23] and [Sn₁₂(μ-O)₂(μ₃-O)₆(μ-OH)₄(OEt)₁₈(μ-OEt)₁₀(HOEt)₄] [24]. In addition the mixed valent Sn(II)/Sn(IV) oxido cluster [Sn₄(μ₄-O)₂(μ₃-OSiMe₃)₂(μ-OSiMe₃)₅(OSiMe₃)₂] was reported [18].

The tin(II) oxido alkoxides offer the possibility to bind transition metal moieties by coordination via the lone pair of electrons of the tin atom. In principle, tin(II) oxido alkoxides can thus be used as starting materials to prepare well-defined heterobimetallic clusters which might serve as single source precursors to heterobimetallic oxide composites. A seminal example for the post-modification strategy was provided by Sita et al., in 1997. Reaction of [Sn₆(μ₃-O)₄(μ₃-OSiMe₃)₄] with [Fe₂(CO)₉] allows the isolation of either [{Sn₆(μ₃-O)₄(μ₃-OSiMe₃)₄}Fe(CO)₄] or [{Sn₆(μ₃-O)₄(μ₃-OSiMe₃)₄}Fe(CO)₄]₂ [17]. Other examples of such heterobimetallic clusters were observed as hydrolysis products starting from mixtures of two metal-containing precursors, e.g. [{Sn₆(μ₃-O)₄(μ₃-OH)₄}Mn(CO)₂Cp^{*}]₆] [25], [{Sn₆(μ₃-O)₄(μ₃-OH)₄}W(CO)₅]₆] [26], [PPPh₄]₂[{Sn₇(μ₃-OH)₄(μ₃-O)₃(μ₃-OEt)₃}W(CO)₅]₇] [26], [Sn₆(μ₃-O)₄(μ₃-OH)₄Cr(CO)₅]₆] [27] and [{Sn₆(μ₃-O)₈}Fe(CO)₂Cp^{*}]₆][AgCl]₂ [28].

Currently we are studying molecular precursors of tin and germanium with potential for the concept of twin polymerization, a process which provides access to novel nanostructured organic-inorganic hybrid materials composed of metal oxides and polymers that can be converted into highly porous materials [23,29,30]. Twin polymerization is defined as a concerted formation of two polymers in one synthetic step starting from a single precursor, which typically bears alkoxide moieties that are suitable for cationic polymerization, e.g. salicyl alcoholates or arylmethanolates [31]. Here, we report for the first time on heterobimetallic tin oxido clusters of such arylmethanolates, which were obtained starting from the corresponding tin(II) alkoxides, e.g. bis(2-methoxyphenylmethanolate)tin(II) (**1**) and bis(2,4-dimethoxyphenylmethanolate)tin(II) (**2**). The starting materials **1** and **2** and the tin oxido clusters [{Sn₆(μ₃-O)₄(μ₃-OCH₂C₆H₄(OCH₃)₂-2,4)}W(CO)₅]₄ (**3**), [{Sn₆(μ₃-O)₄(μ₃-OCH₂C₆H₃(OCH₃)₂-2,4)}W(CO)₅]₄ (**4**) and [{Sn₅(μ₃-O)₂(μ-OCH₂C₆H₃(OCH₃)₂-2,4)₂Fe(CO)₄]₂ (**5**) were characterized by elemental analyses, ATR-IR spectroscopy and NMR spectroscopy in solution as well as in solid state and X-ray single crystal structure analysis (**1**, **4**·2THF and **5**, see Table 1). The syntheses and structures in solution and in the solid state are discussed.

2. Material and methods

All manipulations were carried out under inert atmosphere (N₂ or Ar) using Schlenk techniques. Toluene, *n*-pentane, *n*-hexane and diethyl ether were distilled over sodium. Tetrahydrofuran was dried twice, first over sodium and then over Na/K alloy. Karl-Fischer titration of the solvents gave the following water contents: THF (21.0 ppm), toluene (8.6 ppm), *n*-hexane (1.1 ppm), *n*-pentane (1.1 ppm). Tungsten hexacarbonyl (ABCR 99%), tin(II) chloride, 2-methoxybenzyl alcohol (Alfa Aesar 98%) and 2,4-dimethoxybenzaldehyde (Acros Organics 98%) were used without further purification. Compound **1** [Sn(OCH₂C₆H₄(OCH₃)₂)₂] and compound **2** [Sn(OCH₂C₆H₃(OCH₃)₂-2,4)₂] were synthesized according to a literature procedure [32]. UV-light irradiation was executed by a medium pressure mercury vapor lamp (90 V, Heraeus

Noblelight). ATR-FT-IR spectra were recorded with a BioRad FTS-165 spectrometer with a golden gate sample holder. ¹H and ¹³C {¹H} NMR data were recorded on a Bruker Avance III 500 spectrometer at 500.3 and 125.8 MHz and are referenced to SiMe₄ (δ = 0 ppm). For the ¹¹⁹Sn{¹H} NMR spectra the chemical shifts are reported in ppm relative to SnMe₄ (δ = 0 ppm) and were recorded with a Bruker Avance 400 spectrometer at 111.9 MHz. Solid state NMR measurements were performed at 9.4 T on a Bruker Avance 400 spectrometer equipped with double-tuned probes capable of magic angle spinning (MAS). ¹³C{¹H} CP MAS NMR spectroscopy was accomplished in 4 mm rotors made of zirconium oxide spinning at 12.5 kHz. Cross-polarization with contact times of 3 ms was used to enhance sensitivity. The recycle delay was 5 s. ¹¹⁹Sn{¹H} CP MAS spectroscopy was performed in 4 mm rotors spinning at 12.5 kHz. The recycle delay was 10 s. The spectra were referenced with respect to TMS with tetracyclohexylstannane as a secondary standard (δ 3.6 ppm for ¹³C, δ –97.3 ppm for ¹¹⁹Sn). Melting point evaluation was carried out with a “Melting Point B-540” apparatus from Büchi. Elementary analyses were determined using a vario MICRO from Elementar Analysensysteme GmbH. X-ray powder diffraction measurements were carried out with a STOE-STADI-P diffractometer equipped with a Germanium(111) monochromator and CuK_{α1} radiation (λ = 1.540598 Å, 40 KV, 40 mA).

Single crystal X-ray diffraction data were obtained by using an Oxford Gemini S diffractometer at 110 K (**1** and **5**, CuK_α (λ = 1.54184 Å)) and 100 K (**4**·2THF, Mo K_α (λ = 0.71073 Å)). The structures were solved using SHELXS-2013 and refined by full-matrix least-squares produced on F^2 using SHELXL-2013 [33]. All non-hydrogen atoms were refined anisotropically. All hydrogen atoms were geometrically placed and refined isotropically in riding modes using default parameters. In case of **4**·2THF the atoms C2–C7, C9 and O6 of one, and the atoms C11–C16, C18 and O8 of a second benzylmethanolato ligand were individually refined disordered with split occupancies of 0.43/0.57, respectively.

The figures were created with DIAMOND (release 3.1, 2006) [34]. CCDC 1450431 (**1**), 1450432 (**4**), 1450433 (**5**).

2.1. Synthesis of the tin(II)-tungsten oxido clusters **3**–**5**

2.1.1. [{Sn₆(μ₃-O)₄(μ₃-OCH₂C₆H₄(OCH₃)₂-2,4)}W(CO)₅]₄ (**3**)

A solution of [W(CO)₆] (0.365 g, 1.04 mmol) in 280 ml THF was irradiated with an UV-lamp for 7 h at ambient temperature. The yellow solution was slowly added to a suspension of bis(2-methoxyphenylmethanolate)tin(II) (**1**) (0.410 g, 1.04 mmol) in 20 ml THF and the suspension was left to stir overnight. The reaction mixture was concentrated at reduced pressure until a volume of 50 ml was obtained. Crystallization from reaction solution by gas phase diffusion of *n*-pentane gave compound **3** as pale yellow microcrystals. Yield: 0.245 g (54%); decomp. 130 °C. ¹H NMR (CDCl₃, 500.3 MHz, TMS) δ [ppm] 3.80 (s, 3H, CH₃O), 5.02 (s, 2H, CH₂), 6.66 (d, 1H, ³J_{H,H} = 8.1 Hz), 6.85 (t, 1H, ³J_{H,H} = 7.4 Hz), 7.20 (m, 2H). ¹³C {¹H} NMR (125.81 MHz, CDCl₃, TMS) δ [ppm] 54.3 (OCH₃), 65.1 (CH₂), 110.4, 121.4, 126.7, 130.9, 131.0, 157.3, 196.5 (eq. CO, ¹J(¹⁸³W–¹³C) = 124 Hz), 198.3 (ax. CO). ¹¹⁹Sn{¹H} NMR (CDCl₃, 111.9 MHz, SnMe₄) δ [ppm] –403 [2S_n, ²J(¹¹⁹Sn–¹¹⁷Sn) = 144 Hz], –164 [4S_n, ²J(¹¹⁹Sn–¹¹⁷Sn) = 144 Hz; ¹J(¹¹⁹Sn–¹⁸³W) = 1578 Hz], (as a result of hydrolysis, other minor signals also occurred with main signals at –347 [0.08: 1 (Sn_w), ²J(¹¹⁹Sn–¹¹⁷Sn) = 114 Hz] and –205 [0.16: 1 (Sn_w), ²J(¹¹⁹Sn–¹¹⁷Sn) = 114 Hz]. ¹³C{¹H} CP MAS NMR (100.62 MHz) δ [ppm] 54.1 (br, CH₃O), 64.9 (br, CH₂), 110.7 (br), 122.1 (br), 127.4 (br), 130.7 (br, double intensity), 157.7 (br), 196.1 br, CO).

ATRIR [cm^{-1}]: ν_{CHasym} 2936 (m), ν_{CHsym} 2865 (m), $\nu_{\text{C=O}}$ 2070 (s), $\nu_{\text{C=O}}$ 1989 (w), $\nu_{\text{C=O}}$ 1896 (s), 1603 (m), 1590 (m), 1507 (m), 1491 (m), 1466 (m), 1362 (w), 1320 (w), 1293 (w), 1244 (m), 1178 (w),

Table 1Crystal data of compounds **1**, **4**·2THF and **5**.

Compound	1	4·2THF	5
Empirical formula	C ₁₆ H ₁₈ O ₄ Sn	C ₆₄ H ₆₀ O ₃₈ Sn ₆ W ₄	C ₆₂ H ₆₆ O ₂₈ Sn ₅ Fe ₂
Formula weight [g/mol]	392.99	2884.66	1964.29
Temperature (K)	110	100	110
Wavelength (Å)	1.54184	0.71073	1.54184
Crystal system	monoclinic	monoclinic	monoclinic
Space group	P2 ₁ /c	C2/c	C2/c
<i>a</i> (Å)	5.9124(4)	24.2721(7)	25.4728(5)
<i>b</i> (Å)	10.7542(8)	15.6967(3)	9.2010(2)
<i>c</i> (Å)	24.537(2)	25.3331(8)	29.0478(8)
α (°)	90	90	90
β (°)	96.674(7)	114.292(4)	92.446(2)
χ (°)	90	90	90
<i>V</i> (Å ³)	1549.5(2)	8797.1(5)	6801.9(3)
<i>Z</i>	4	4	4
<i>D</i> _{calcd} (g/cm ³)	1.685	2.178	1.918
Absorption coefficient [mm ⁻¹]	13.234	6.960	18.414
<i>F</i> (000)	784	5376	3856
Theta range for data collection [°]	3.63 to 62.70	2.90 to 25.00	3.05 to 67.73
Limiting indices	-6 ≤ <i>h</i> ≤ 6 -10 ≤ <i>k</i> ≤ 12 -27 ≤ <i>l</i> ≤ 28	-27 ≤ <i>h</i> ≤ 28 -11 ≤ <i>k</i> ≤ 18 -30 ≤ <i>l</i> ≤ 30	-30 ≤ <i>h</i> ≤ 22 -9 ≤ <i>k</i> ≤ 10 -34 ≤ <i>l</i> ≤ 26
No. of reflections collected	7721	19755	11965
No. of unique reflections/ <i>R</i> _{int}	2449/0.0697	7726/0.0328	6028/0.0372
Final <i>R</i> indices [<i>I</i> > 2σ(<i>I</i>)] ²	<i>R</i> ₁ = 0.0445 w <i>R</i> ₂ = 0.1063	<i>R</i> ₁ = 0.0317 w <i>R</i> ₂ = 0.0716	<i>R</i> ₁ = 0.0609 w <i>R</i> ₂ = 0.1613
<i>R</i> indices (all data)	<i>R</i> ₁ = 0.0670 w <i>R</i> ₂ = 0.1138	<i>R</i> ₁ = 0.0400 w <i>R</i> ₂ = 0.0747	<i>R</i> ₁ = 0.0688 w <i>R</i> ₂ = 0.1681
Goodness-of-fit on <i>F</i> ²	0.912	1.039	1.060
Largest diff. peak/ hole [eÅ ⁻³]	1.393 / -1.183	1.405 / -1.205	2.609 / -1.274

1123 (m), 1021 (m), 965 (m), 934 (m), 857 (w), 837 (w), 751 (s), 625 (s), $\nu_{\text{Sn}-\text{O}}$ 563 (s). CHN analysis calcd (%) for C₅₂H₃₆O₃₂Sn₆W₄: C, 23.8; H, 1.4; found: C, 23.5; H, 1.4.

2.1.2. $\left[\{\text{Sn}_6(\mu_3\text{-O})_4(\mu_3\text{-OCH}_2\text{C}_6\text{H}_3(\text{OCH}_3)_2\text{-}2,4)_4\}\{\text{W}(\text{CO})_5\}_4\right]$ (**4**)

Compound **4** was prepared according to the protocol for **3** starting from [W(CO)₆] (0.365 g, 1.04 mmol) and bis(2,4-dimethoxyphenylmethanolate)tin(II) (**2**) (0.470 g, 1.04 mmol) in 280 ml THF. After three days, compound **4** crystallized as **4**·2THF at ambient temperature. Yield: 0.215 g (33%); decomp. 128 °C. ¹³C{¹H} CP MAS NMR (100.62 MHz) δ [ppm] 25.3 (CH₂ THF) 54.3 (CH₃O), 54.8 (CH₃O, double intensity), 55.7 (CH₃O), 65.0 (CH₂), 65.6, 67.3 (OCH₂ THF), 100.0, 101.0, 103.2, 103.6, 119.3, 119.9, 131.5, 132.0, 158.2, 159.2, 162.3, 162.8, 195.3–200.5 (br, CO). ATR IR [cm⁻¹]: ν_{CHasym} 2936 (m), ν_{CHsym} 2863 (m), $\nu_{\text{C=O}}$ 2070 (s), $\nu_{\text{C=O}}$ 1983 (m), $\nu_{\text{C=O}}$ 1898 (s), 1613 (m), 1588 (m), 1507 (m), 1464 (m), 1364 (w), 1331 (w), 1291 (m), 1266 (m), 1208 (s), 1132 (s), 1028 (s), 961 (m), 932 (m), 833 (m), 617 (s), $\nu_{\text{Sn}-\text{O}}$ 558 (s). CHN analysis calcd (%) for C₆₄H₆₀O₃₈Sn₆W₄: C, 26.7; H, 2.1; found: C, 26.6, H, 2.0.

2.1.3. $\left[\{\text{Sn}_5(\mu_3\text{-O})_2(\mu\text{-OCH}_2\text{C}_6\text{H}_3(\text{OCH}_3)_2\text{-}2,4)_4\}(\mu_3\text{-OCH}_2\text{C}_6\text{H}_3(\text{OCH}_3)_2\text{-}2,4)_2\}\{\text{Fe}(\text{CO})_4\}_2\right]$ (**5**)

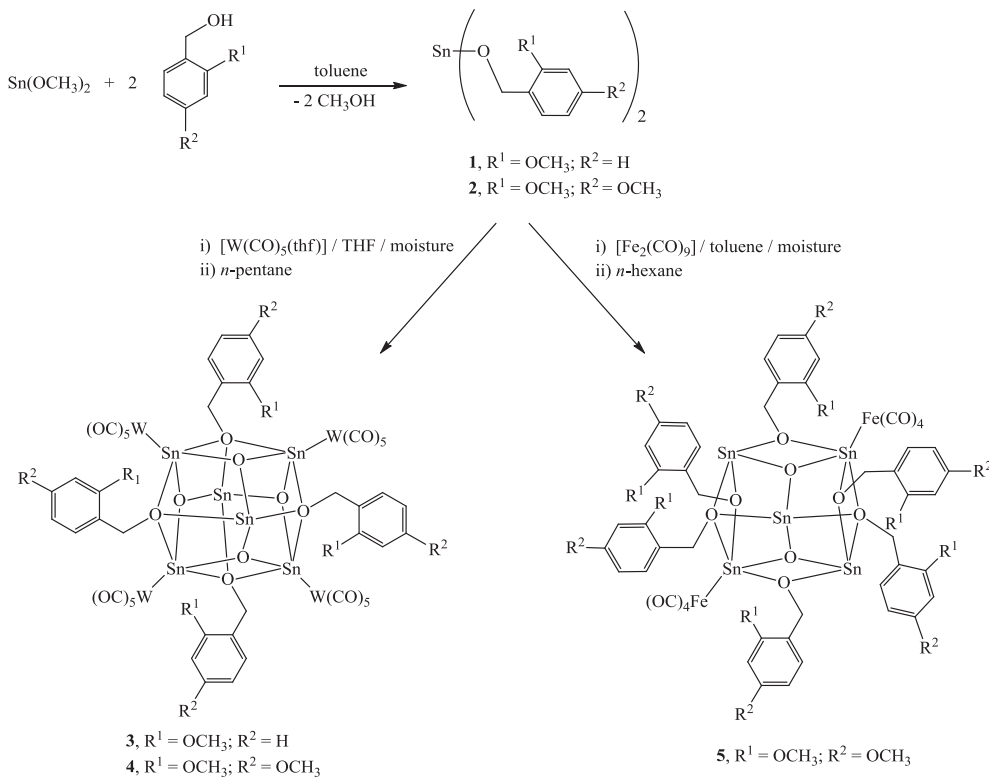
A solution of [Fe₂(CO)₉] (0.21 g, 0.59 mmol) in 50 ml of toluene was added to a suspension of bis(2,4-dimethoxyphenylmethanolate)tin(II) (**2**) (0.53 g, 1.18 mmol) in 30 ml of toluene. The mixture was heated at 60 °C until a clear solution was obtained. After cooling to room temperature the reaction mixture was filtered over celite and the obtained orange solution was concentrated at reduced pressure until a volume of 30 ml was obtained. Finally diffusion of *n*-hexane via the gas phase afforded compound **5** after one week as yellow crystals. Yield: 0.280 g (60%); decomp. 145 °C. ¹H NMR (C₆D₆, 500.3 MHz, TMS) δ [ppm] 3.20 (s, OCH₃, 6H), 3.28 (s, OCH₃, 6H), 3.34 (s, OCH₃, 6H), 3.35 (s, OCH₃, 6H), 3.40 (s, OCH₃, 6H), 3.47 (s, OCH₃, 6H), 4.97, AB spin system with δ_A = 4.87 and δ_B = 5.07 (4H, CH₂ $^2J_{\text{H,H}} = 11.5$ Hz),

5.58, AB spin system with δ_A = 5.42 and δ_B = 5.72 (4H, CH₂, $^2J_{\text{H,H}} = 11.1$ Hz), 5.51, AB spin system with δ_A = 5.48 and δ_B = 5.54 (4H, CH₂, $^2J_{\text{H,H}} = 12.8$ Hz), 6.10 (dd, 2H, $^3J_{\text{H,H}} = 8.2$ Hz, $^4J_{\text{H,H}} = 2.2$ Hz), 6.30 (m, 6H), 6.48 (dd, 2H, $^3J_{\text{H,H}} = 8.2$ Hz, $^4J_{\text{H,H}} = 2.3$ Hz), 6.52 (d, 2H, $^3J_{\text{H,H}} = 2.2$ Hz), 7.20 (d, 2H, $^3J_{\text{H,H}} = 8.3$ Hz), 7.31 (d, 2H, $^3J_{\text{H,H}} = 8.2$ Hz), 7.45 (d, 2H, $^3J_{\text{H,H}} = 8.2$ Hz). ¹³C{¹H} NMR (125.81 MHz, C₆D₆, TMS) δ [ppm] 54.3 (OCH₃), 54.4 (OCH₃), 54.7 (OCH₃), 54.9 (OCH₃), 55.0 (OCH₃), 55.1 (OCH₃), 60.6 (CH₂), 63.3 (CH₂), 63.8 (CH₂), 98.9, 99.0, 99.6, 103.9, 104.2, 104.4, 121.1, 123.4, 123.7, 131.7, 132.0, 132.3, 159.1, 159.3, 159.6, 161.7, 161.9, 162.3, 215.8 (eq. CO), 216.4 (ax. CO). ¹¹⁹Sn{¹H} NMR (C₆D₆, 111.9 MHz, SnMe₄): δ [ppm] -445 (25n), -396 (15n), -74 (2Sn_{Fe}). ATR IR [cm⁻¹]: ν_{CHasym} 2938 (m), ν_{CHsym} 2841 (m), $\nu_{\text{C=O}}$ 2026 (s), $\nu_{\text{C=O}}$ 1943 (w), $\nu_{\text{C=O}}$ 1904 (s), 1611 (s), 1586 (s), 1505 (s), 1455 (s), 1437 (m), 1420 (m), 1368 (w), 1333 (m), 1287 (s), 1262 (s), 1239 (w), 1208 (s), 1156 (s), 1131 (s), 1032 (s), 1009 (s), 978 (s), 963 (s), 930 (s), 918 (s), 833 (m), 812 (s), 784 (s), 737 (w), 712 (w), 648, (m), $\nu_{\text{Sn}-\text{O}}$ 617 (s), 560 (s), 534 (s), 475 (s). CHN analysis calcd (%) for C₆₂H₆₆O₂₈Sn₅Fe₂: C, 37.9; H, 3.4; found: C, 37.6; H, 3.3.

3. Results and discussion

The reaction between tin(II) methoxide and two equivalents of 2-methoxybenzyl alcohol and 2,4-dimethoxybenzyl alcohol, respectively, in toluene at 80 °C afforded bis(2-methoxyphenylmethanolate)tin(II) (**1**) and bis(2,4-dimethoxyphenylmethanolate)tin(II) (**2**) (Scheme 1).

Compounds **1** and **2** are poorly soluble in toluene, THF, CHCl₃ and CH₂Cl₂ and when left in solution for 2 h in the presence of moisture they hydrolyse to give the starting alcohol and insoluble inorganic material. Single crystals suitable for X-ray diffraction were obtained after dissolving **1** at 80 °C in toluene and cooling of the solution to room temperature. An one-dimensional (1D) coordination polymer with tetra-coordinated tin atoms is observed in the crystal of **1**, which is a result of the asymmetric bridging



Scheme 1. Synthesis pathway to the decanuclear heterobimetallic tin(II)-tungsten oxido clusters **3** and **4** and the heptanuclear heterobimetallic tin(II)-iron oxido cluster **5**.

behavior of each benzylalcoholato ligand via its oxygen atom (**Fig. 1**). The covalent and coordinative bond distances [Sn1–O1 2.12(5) Å, Sn1–O3 2.13(5) Å and Sn1–O1A 2.35(4) Å, Sn1–O3B 2.31(4) Å] and O–Sn–O angles (O1–Sn1–O3 91.1(2)° and O1A–Sn1–O3B 154.8(2)°] are in good agreement with a *pseudo* trigonal bipyramidal geometry of the type SnO₄E that includes a stereochemically active lone pair of electrons E. The methoxy groups are located at large distances (Sn···OMe from 4.56 Å–5.80 Å) and thus are not coordinated to the tin atoms. The structure of **1** in the solid state is close to that of Sn(OR)₂ [R=*neo*Pent; Sn–O 2.113(3)–2.403(3) Å], with slightly elongated intermolecular coordinative Sn–O bonds in the latter [16].

ATR-IR spectra in the solid state of **1** and **2** are quite similar, revealing characteristic strong absorption bands for **1** and **2** (ν_{C-O} and ν_{Sn-O}). Absorption bands corresponding to OH groups were not detected. However in the presence of moisture the alkoxides easily hydrolyse to the corresponding alcohol. Thus broad and intensive OH groups were observed after storage of the compounds under ambient conditions for a couple of minutes.

The assumption that both compounds **1** and **2** exhibit similar molecular structures is corroborated by solid state $^{119}\text{Sn}\{^1\text{H}\}$ CP MAS NMR. Compound **1** reveals a chemical shift at δ –351 ppm and compound **2** at δ –350 ppm consistent with a SnO_4 environment. These values are in a good agreement with those found in case of tetra-coordinated metal atoms in tin alkoxides, e.g. $\text{Sn}(\text{OtBu})_4$ (δ –367 ppm), $\text{Sn}(\text{OtPent})_4$ (δ –370 ppm) and the tris-stannylene $[\text{Sn}(\text{O}_2\text{C}_6\text{H}_4-1,2)_2\{\text{SnN}(\text{SiMe}_3)_2\}]$ [δ –388 (SnO_4 core) and 7 ppm (SnO_2N core)] [8,35–37]. In accordance with the literature compounds **1** and **2** gave eight and nine $^{13}\text{C}\{^1\text{H}\}$ NMR resonances, respectively [32]. ^1H NMR spectroscopy in solution shows broad singlet resonance signals for **1** and **2** which point to equilibria between monomeric and oligomeric species for both compounds in solution. This assumption is confirmed by $^{119}\text{Sn}\{^1\text{H}\}$ NMR in CDCl_3 ,

Two resonance signals at δ -272 and -161 ppm (1:7 integral ratio) were observed for **1** and at δ -270 and -162 ppm (2:9 integral ratio) for **2**, with the latter being of higher solubility. These values do not correspond to the $^{119}\text{Sn}\{^1\text{H}\}$ NMR chemical shifts in the solid state, which are located at ca. δ -350 ppm for both compounds as a result of tetra-coordinated tin atoms. The $^{119}\text{Sn}\{^1\text{H}\}$ NMR signals at ca. δ -160 ppm are indicative for the presence of two-coordinated tin atoms whereas those at ca. δ -270 ppm indicate a three-coordinated SnO_3 core, which most likely results from dimerisation. Similar chemical shifts were observed for two-coordinated tin atoms in $\text{Sn}(\text{OC}t\text{Bu}_3)_2$ (δ -163 ppm) [38] and three-coordinated tin atoms in $[\text{Sn}(\text{u-OiPr})(\text{OSiPh}_3)]_2$ (δ -246 ppm) [39].

Reactions of the tin(II) alkoxides with $[W(CO)_5(thf)]$ (for **1** and **2**) in THF and $[Fe_2(CO)_9]$ in toluene (for **2**) did not provide heterobimetallic dinuclear coordination complexes but gave reproducibly the decanuclear tin(II)-tungsten oxido clusters $\{[Sn_6(\mu_3-O)_4(\mu_3-OCH_2R)_4]\{W(CO)_5\}_4\}$ (**3**, R=C₆H₄(OCH₃)-2; **4**, R=C₆H₃(OCH₃)₂-2,4] and the heptanuclear tin(II)-iron oxido cluster $\{[Sn_5(\mu_3-O)_2(\mu-OCH_2R)_4(\mu_3-OCH_2R)_2]\{Fe(CO)_4\}_2\}$ (**5**, R=C₆H₃(OCH₃)₂-2,4] in fair yield (**3**: 54%; **4**: 2THF: 33%, **5**: 60%). All clusters are a result of partial hydrolysis which is attributed to residual water in the solvents (THF 21 ppm; toluene 8.6 ppm). Noteworthy, starting from the suspensions of the tin(II) alkoxides the reaction mixture turns into a solution only if water is present but its amount must be kept in the low ppm region to prevent formation of hydrolysis products of low solubility. When using lower volumes of THF (30 ml instead of 300 ml) or toluene (20 ml instead of 80 ml) the alkoxides do not dissolve, but when small amounts of solvent (ca. 5%) with a higher concentration of water was added (THF 200 ppm; toluene 65 ppm), the alkoxides solubilised immediately. When the syntheses were performed with lower volumes of THF (30 ml with 220 ppm water) and toluene (20 ml with 65 ppm water) the alkoxides did undergo

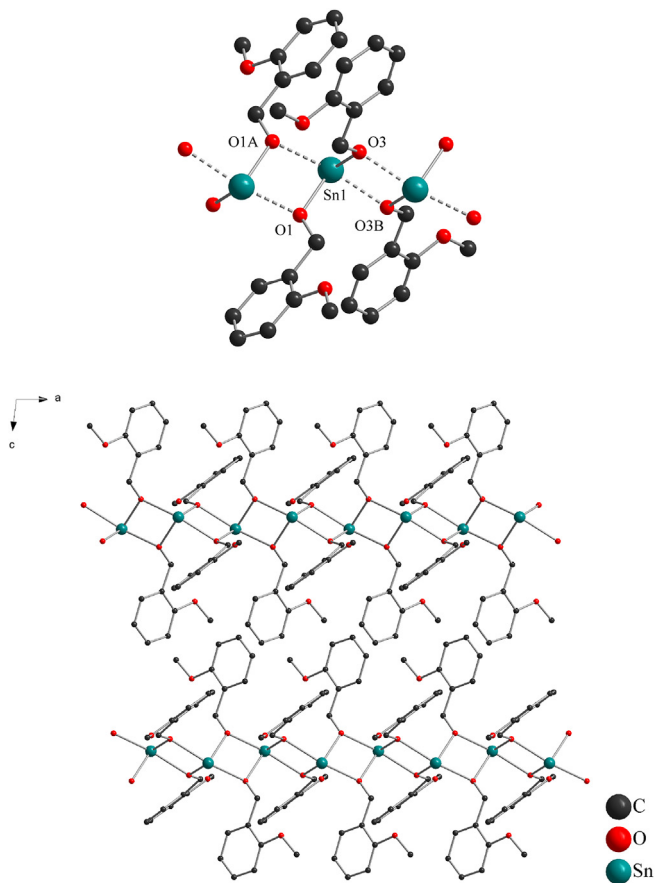


Fig. 1. Ball-and-stick model of a fragment of the polymeric chain of **1** (up) and plot of the packing diagram of **1** (down). For clarity, hydrogen atoms are omitted. Selected bond lengths [Å] and angles [°]: Sn1–O1 2.12(5), Sn1–O3 2.13(5), Sn1–O1A 2.35(4), Sn1–O3B 2.31(4), O1–Sn1–O(3) 91.1(2), O1–Sn1–O3B 88.5(2), O1–Sn1–O1A 73.6(2), O3–Sn1–O1A 88.8(2), O3–Sn1–O3B 73.7(2), O1A–Sn1–O3B 154.8(2). Symmetry transformations used to generate equivalent atoms: 'A' = $-x + 1, -y + 2, -z + 2$. 'B' = $-x, -y + 2, -z + 2$.

hydrolysis to give insoluble amorphous materials instead of clusters. Compounds **3** and **4** were crystallized from THF by diffusion of *n*-pentane via the gas phase into a concentrated reaction solution. For **3** a polycrystalline material was obtained, which was not suitable for single crystal X-ray diffraction due to very small domain sizes. By contrast compound **4** gave crystals of higher quality and structure elucidation revealed the decanuclear tin(II)-tungsten oxido cluster **4**·2THF with disordered benzylmethanolato ligands. Both compounds **3** and **4**, respectively, are assumed to form decanuclear tin(II)-tungsten oxido clusters with a hexanuclear tin(II) oxido core structure embedded by four tungsten pentacarbonyl units and four alkoxido ligands. In Fig. 2 the molecular structure of **4** is given.

The oxido cluster **4** possesses crystallographically imposed C_2 symmetry, with the C_2 axis going through the tin atoms Sn3 and Sn4. The tin(II) oxido core is best described as an octahedron with the tin atoms occupying the corners and four μ_3 -oxido and four μ_3 -alkoxido ligands occupying the eight faces. The four bulky alkoxido ligands are orientated along the crystallographic *b*-axis and prevent any additional coordination to Sn3 and Sn4. Thus, these tin atoms exhibit a distorted pseudo-trigonal bipyramidal coordination geometry of the type $\text{Sn}_4\text{O}_6\text{E}$ including a stereochemically active lone pair of electrons E. The distortion is manifested in the O4–Sn3–O4A angle of 129.9(2)° (apical positions) and by two types of tin–oxygen distances, corresponding to short equatorial

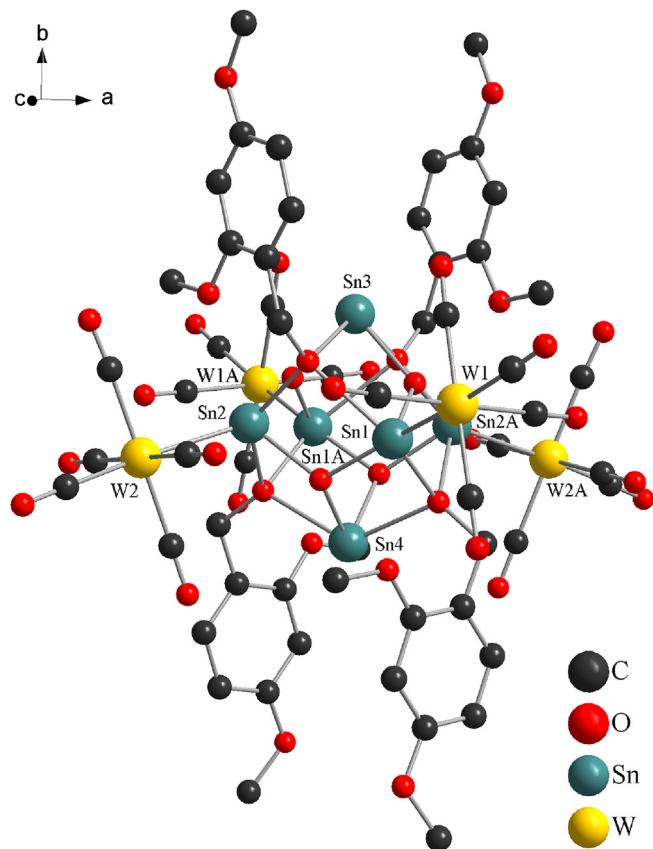


Fig. 2. Molecular structure of the heterobimetallic tin(II)-tungsten oxido cluster **4** as ball-and-stick model. For clarity, all hydrogen atoms are omitted and of disordered atoms only one atomic position is displayed. Symmetry transformations used to generate equivalent atoms: 'A' = $-x + 1, y, -z + \frac{1}{2}$.

bonds [Sn3–O1 2.12(4) Å, Sn4–O2 2.12(4) Å] and others, which are significantly longer [Sn3–O4 2.44(4) Å, Sn4–O3 2.43(4) Å]. The other tin atoms coordinate each to a $\text{W}(\text{CO})_5$ -unit with bond distances Sn1–W1 2.727(5) Å and Sn2–W2 2.739(5) Å, which is well in line with reported tin-tungsten complexes [26,40–47]. As a result of this interaction and additional intramolecular tin–oxygen coordination by the alkoxido ligand the coordination geometry of the tin atoms Sn1 and Sn2 (and the symmetry related tin atoms) is best described as mono-capped trigonal bipyramidal $\text{O}\rightarrow\text{Sn}_4\text{O}_6\text{W}$ (Fig. 3). The corresponding Sn1–O bond distances cover the range Sn1–O1 2.06(4) Å, Sn1–O2A 2.04(4) Å, Sn1–O3 2.19(4) Å to Sn1–O4A 2.51(4) Å and similar values are found for the other corresponding tin atoms of the octahedron. The additional intramolecular tin–oxygen distances related to the ligand are found in the range from 2.94(5) Å to 2.99(5) Å, which is significantly below the sum of the van der Waals radii of tin and oxygen [$\Sigma r_{\text{vdw}}(\text{Sn}, \text{O})$] 3.69 Å [48]. The $\text{Sn}\rightarrow\text{W}(\text{CO})_5$ fragments show a distorted octahedral symmetry and the OC–W–CO angles are in the range of 87.4(3)°–92.5(3)° for the orthogonal groups and in the range of 178.5(3)°–179.6(3)° for the almost linearly arranged OC–W–CO groups.

Powder X-ray diffraction analysis of bulk **4**·2THF confirms phase purity and that of bulk **3** confirms its polycrystalline nature. The ^{13}C { ^1H } CP MAS NMR study of the almost insoluble compound **4**·2THF shows, as expected from the single crystal X-ray diffraction data, two environments for the organic ligands and gave 12 resonance signals for the aromatic carbon atoms, two signals for the methylene groups, three signals (one signal of double intensity due to

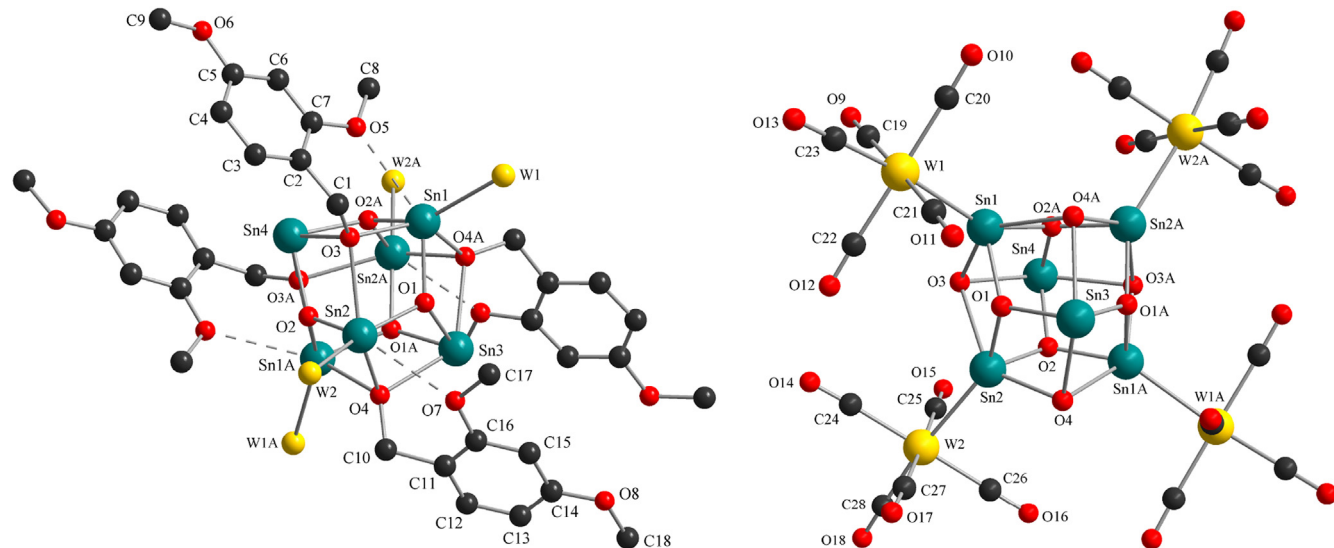


Fig. 3. The tin(II) oxido alkoxido core in the molecular structure of **4** showing the additional intramolecular tin-oxygen coordination [only the coordinated tungsten atoms are shown] (left), and the tin(II)-oxygen core with coordinated $\text{W}(\text{CO})_5$ units for the same compound [the organic part of the alkoxido ligands is not shown] (right). For clarity, all hydrogen atoms are omitted and of disordered atoms only one atomic position is displayed. Selected bond lengths [\AA] and angles [$^\circ$]: Sn_1-O_1 2.06(4), $\text{Sn}_1-\text{O}_2\text{A}$ 2.04(4), Sn_1-O_3 2.19 (4), $\text{Sn}_1-\text{O}_4\text{A}$ 2.51(4), Sn_2-O_1 2.03(4), $\text{Sn}_2-\text{O}_2\text{A}$ 2.05(4), Sn_2-O_3 2.49(4), Sn_2-O_4 2.19(4), Sn_3-O_1 2.12(4), Sn_3-O_4 2.44(4), Sn_4-O_2 2.12(4), Sn_4-O_3 2.43(4), Sn_1-O_5 2.94(5), Sn_2-O_7 2.99(5), Sn_1-W_1 2.727(5), Sn_2-W_2 2.739(5), $\text{O}_1-\text{Sn}_1-\text{O}_2\text{A}$ 95.7(2), $\text{O}_1-\text{Sn}_1-\text{O}_3$ 77.9(2), $\text{O}_1-\text{Sn}_1-\text{O}_4\text{A}$ 73.4 (1), $\text{O}_2\text{A}-\text{Sn}_1-\text{O}_3$ 78.5(2), $\text{O}_2\text{A}-\text{Sn}_1-\text{O}_4\text{A}$ 71.5(2), $\text{O}_3-\text{Sn}_1-\text{O}_4\text{A}$ 135.6(1), $\text{O}_1-\text{Sn}_2-\text{O}_2$ 95.9(2), $\text{O}_1-\text{Sn}_2-\text{O}_3$ 71.7(2), $\text{O}_1-\text{Sn}_2-\text{O}_4$ 78.3(2), $\text{O}_2-\text{Sn}_2-\text{O}_3$ 73.5(1), $\text{O}_2-\text{Sn}_2-\text{O}_4$ 78.4(2), $\text{O}_3-\text{Sn}_2-\text{O}_4$ 135.90(1), $\text{O}_1-\text{Sn}_3-\text{O}_1\text{A}$ 91.1(2), $\text{O}_1-\text{Sn}_3-\text{O}_4$ 71.4(1), $\text{O}_1-\text{Sn}_3-\text{O}_4\text{A}$ 74.1(1), $\text{O}_4-\text{Sn}_3-\text{O}_4\text{A}$ 129.9(2), $\text{O}_2-\text{Sn}_4-\text{O}_2\text{A}$ 92.0(2), $\text{O}_2-\text{Sn}_4-\text{O}_3$ 73.8(1), $\text{O}_2-\text{Sn}_4-\text{O}_3\text{A}$ 71.9(2), $\text{O}_3-\text{Sn}_4-\text{O}_3\text{A}$ 129.6(2). Symmetry transformations used to generate equivalent atoms: 'A' = $-x + 1, y, -z + \frac{1}{2}$.

overlap of two signals) for the carbon atoms of the methoxy groups, two signals for the THF molecules and one broad signal for the carbon atoms of the $\text{W}(\text{CO})_5$ -unit. In comparison to compound **4** (single crystals) the $^{13}\text{C}\{^1\text{H}\}$ CP MAS NMR spectrum of compound **3** (polycrystalline) shows one set of broader signals, that includes 5 distinguished resonance signals for the aromatic carbon atoms (one signal of double intensity due to overlap of two signals), one signal for the methylene groups, one signal for the methoxy groups and one broad signal for the $\text{W}(\text{CO})_5$ fragments.

^1H NMR spectroscopic analysis of **3** in CDCl_3 solution gave five resonance signals showing an integral ratio of 3:2:1:1:2. The $^{13}\text{C}\{^1\text{H}\}$ NMR spectrum of **3** in CDCl_3 solution shows one set of resonance signals which indicates that all of the four alkoxido ligands are chemical equivalent. $^{119}\text{Sn}\{^1\text{H}\}$ NMR spectroscopy gave two signals at δ –164 and –403 ppm with an integral ration of 2:1. The value of $^2J(^{119}\text{Sn}-^{117}\text{Sn})$ = 144 Hz is in good agreement with the literature value for $[\{\text{Sn}_2(\mu\text{-OtBu})_2(\text{OtBu})_2\}\{\text{W}(\text{CO})_5\}_2]$ [$^2J(^{119}\text{Sn}-^{117}\text{Sn})$ = 137 Hz] [45]. In addition the resonance signal at δ –164 ppm shows $^1J(^{119}\text{Sn}-^{183}\text{W})$ = 1578 Hz which corresponds to values as reported for complexes such as $[\{\text{Sn}_2(\mu\text{-OCMe}_2\text{-CH}_2)(\text{OCH}_2\text{CH}_2)\text{NCH}_2\text{CH}_2\text{NMe}_2\}_2\{\text{W}(\text{CO})_5\}_2]$ [$^1J(^{119}\text{Sn}-^{183}\text{W})$ = 1556 Hz] and $[\{\text{Sn}_2(\mu\text{-OtBu})_2(\text{OtBu})_2\}\{\text{W}(\text{CO})_5\}_2]$ [$^1J(^{119}\text{Sn}-^{183}\text{W})$ = 1485 Hz] [40,45]. The signal is assigned to the four $(\text{CO})_5\text{W}$ -coordinated tin atoms whereas the signal at δ –403 ppm is assigned to the tetra-coordinated tin atoms in trans-position of an elongated octahedral $\{\text{Sn}_6\}$ -unit. Noteworthy, in the $^{119}\text{Sn}\{^1\text{H}\}$ NMR spectrum which was measured overnight (9 h) signals of minor intensity did occur as a result of side reactions such as hydrolysis. One additional pair of $^{119}\text{Sn}\{^1\text{H}\}$ NMR signals was observed at δ –205 and –347 ppm with an integral ratio of 2:1 and $^2J(^{119}\text{Sn}-^{117}\text{Sn})$ = 114 Hz, which might indicate the formation of the hexanuclear tin oxido cluster $[\{\text{Sn}_6(\mu_3\text{-O})_4(\mu_3\text{-OH})_4\}\{\text{W}(\text{CO})_5\}_4]$. After one week the intensity of the major signals decreased and more than 15 new signals appeared, demonstrating the hydrolytic instability of **3**.

The ATR-IR spectrum of **3** shows similar CO absorption bands as

observed for **4**·2THF providing further support for our assumption that compound **3** adopts a similar structure as it is observed for compound **4**. Additionally, the CH analysis of the polycrystalline material of **3** is in line with the expected composition of a decanuclear Sn_6W_4 oxido alkoxido cluster.

Single crystals of the tin-iron cluster $[\{\text{Sn}_5(\mu_3\text{-O})_2(\mu\text{-OCH}_2\text{C}_6\text{H}_3(\text{OCH}_3)_2\text{-}2,4)_4\}(\mu_3\text{-OCH}_2\text{C}_6\text{H}_3(\text{OCH}_3)_2\text{-}2,4)_2]\{\text{Fe}(\text{CO})_4\}_2$ (**5**) suitable for X-ray diffraction analysis were obtained by diffusion of *n*-hexane via the gas phase into a concentrated toluene solution. Phase purity was confirmed by PXRD.

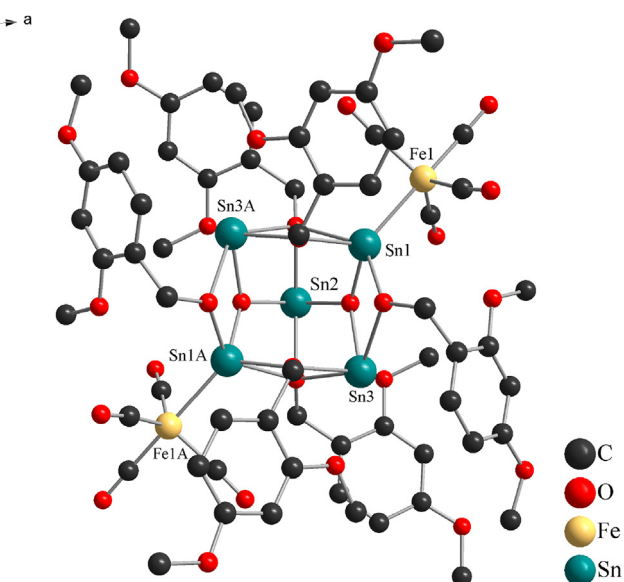


Fig. 4. Molecular structure of the heterobimetallic tin(II)-iron oxido alkoxido cluster **5** in ball-and-stick style. For clarity, all hydrogen atoms are omitted. Symmetry transformations used to generate equivalent atoms: 'A' = $-x, y, -z + \frac{1}{2}$.

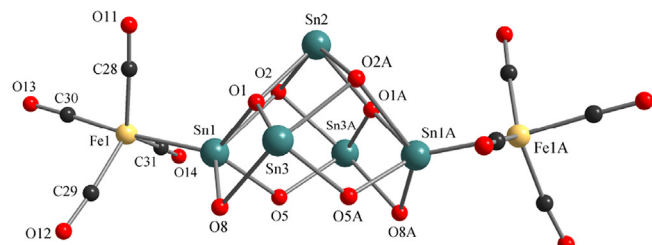
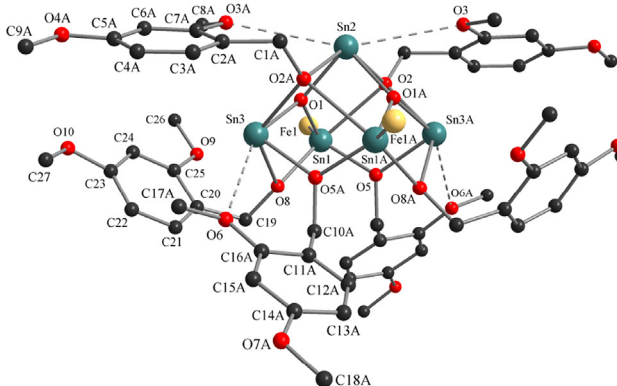


Fig. 5. The tin(II) oxido alkoxido core in the molecular structure of **5** showing the additional intramolecular tin-oxygen coordination [only the coordinated iron atoms are shown] (left), and the tin(II)-oxygen core with coordinated $\text{Fe}(\text{CO})_4$ -units for the same compound [the organic part of the alkoxido ligands is not shown] (right). For clarity, all hydrogen atoms are omitted. Selected bond length [\AA] and angles [$^\circ$]: Sn2–O1 2.08(5), Sn2–O2 2.35(6), Sn1–Fe1 2.483(1), Sn1–O1 1.99(5), Sn1–O2 2.54(5), Sn1–O5 2.06(4), Sn1–O8 2.09(5), Sn3–O1 2.12(5), Sn3–O2A 2.30(5), Sn3–O5A 2.18(5), Sn3–O8 2.46(5), O1–Sn2–O1A 92.8(3), O1–Sn2–O2 74.1(2), O1A–Sn2–O2 73.3(2), O2–Sn2–O2A 132.0(3), O1–Sn1–O2 71.4(2), O1–Sn1–O5 100.2(2), O1–Sn1–O8 78.2(2), O2–Sn1–O5 69.2(2), O2–Sn1–O8 136.7(2), O5–Sn1–O8 87.1(2), O1–Sn3–O2A 73.8(2), O1–Sn3–O5A 94.7(2), O1–Sn3–O8 68.0(2), O2A–Sn3–O5A 72.2(2), O2A–Sn3–O8 130.2(2), O5A–Sn3–O8 80.2(2). Symmetry transformations used to generate equivalent atoms: 'A' = $-x, y, -z + \frac{1}{2}$.

Heptanuclear **5** possesses crystallographically imposed C_2 symmetry, with the C_2 axes going through the Sn2 atom along the crystallographic b -axes (Fig. 4). The inorganic core of **5** contains five tin atoms that occupy the vertices of a square-pyramidal polyhedron and two $\text{Fe}(\text{CO})_4$ -units that are coordinated to two of the tin atoms (Figs. 4 and 5). Two μ_3 -oxido and two μ_3 -alkoxido ligands are placed above the four trigonal faces and the tin atoms of the basal plane are bridged by μ -alkoxido ligands. The tin atoms Sn2 and Sn3 exhibit a distorted pseudo-trigonal bipyramidal coordination geometry of the type SnO_4E assuming a stereochemically active lone pair of electrons E. The tin-oxygen bond distances amount to Sn2–O1 2.08(5) \AA and Sn2–O2 2.35(6) \AA for the apical tin atom and the Sn3 atoms of the square plane show the following Sn–O distances: Sn3–O1 2.12(5) \AA , Sn3–O2A 2.30(5) \AA , Sn3–O5A 2.18(5) \AA and Sn3–O8 2.46(5) \AA . In addition the tin atom at the top of the square pyramid [Sn2 \cdots O3/O3A 3.17(5) \AA] and two tin atoms of the basal plane [Sn3 \cdots O6 3.34(5) \AA , Sn3A \cdots O6A 3.34(5) \AA] exhibit distances to methoxy groups of the ligands that are shorter than the sum of the van der Waals radii [$\Sigma r_{\text{vdW}}(\text{Sn},\text{O})$ 3.69 \AA] [48], which might be interpreted as weak intramolecular stabilisation. Two tin atoms Sn1/Sn1A at trans-basal positions of the polyhedron are coordinated to $\text{Fe}(\text{CO})_4$ moieties with a Sn–Fe bond distance of 2.483(1) \AA , which is comparable with the tin–iron bond lengths, e.g. in the heptanuclear $\{[\text{Sn}_6(\mu_3\text{-O})(\mu_3\text{-OSiMe}_3)_4]\{\text{Fe}(\text{CO})_4\}\}$ [Sn–Fe 2.47 (3) \AA] [17] or octanuclear $\{[\text{Sn}_6(\mu_3\text{-O})(\mu_3\text{-OSiMe}_3)_4]\{\text{Fe}(\text{CO})_4\}_2\}$ [Sn–Fe 2.46(2) \AA] [17] tin–iron oxido clusters and other tin(II)–iron complexes, e.g. $\{[\text{Sn}(\mu\text{-OCMe}_2\text{CH}_2)\text{OCMe}_2\text{CH}_2]\text{NMe}_2\}_2\{\text{Fe}(\text{CO})_4\}_2\}$ [Sn–Fe 2.498(5) \AA] [49] and $\{[\text{SnCl}(\text{RNClMe})_2\text{CH}\{\text{Fe}(\text{CO})_4\}]\}$ [$\text{R}=\text{C}_6\text{H}_3(\text{iPr})_2\text{-}2,6$] [Sn–Fe 2.482 (7) \AA] [50]. The coordination geometry at Sn1 is best described as distorted trigonal bipyramidal (SnO_4Fe core). The Sn– $\text{Fe}(\text{CO})_4$ fragments show a distorted trigonal bipyramidal geometry and the OC–Fe–CO angles are in the range from 91.3(4) $^\circ$ –92.7(3) $^\circ$ and 114.3(4) $^\circ$ –124.5(4) $^\circ$.

Compound **5** is soluble in solvents such as benzene, toluene, chloroform and dichloromethane and the NMR spectra were recorded in C_6D_6 . The $^{119}\text{Sn}\{^1\text{H}\}$ NMR spectrum gave three signals at δ –74, –396 and –445 ppm with an integral ratio of 2:1:2. The resonance signal δ –74 ppm is assigned to penta-coordinated Sn(1), which is bound to $\text{Fe}(\text{CO})_4$ and shows a SnO_4Fe coordination environment. The $^{119}\text{Sn}\{^1\text{H}\}$ NMR chemical shift is in agreement with the value given by Sita et al. for the tin atoms bound to iron in the tin–iron oxido cluster $\{[\text{Sn}_6(\mu_3\text{-O})(\mu_3\text{-OSiMe}_3)_4]\{\text{Fe}(\text{CO})_4\}_2\}$

(δ_{SnFe} –42 ppm) [17]. The tin atom Sn2 which is placed at the top of the square pyramid gave a chemical shift δ –396 ppm whereas the tin atoms Sn3 and Sn3A result in a resonance signal at δ –445 ppm. These values are in accordance with those of $[\text{Sn}(\mu\text{-OC}_6\text{H}_4\text{iPr}-2)_2]_n$ (δ –429, –490 ppm) and compound **3** (δ –408 ppm) and are typical for a SnO_4E coordination environment [51]. However, the upfield shift for Sn3 and Sn3A points to additional weak intramolecular coordination by a methoxy group of an alkoxido ligand. The assumption of such an intramolecular coordination is also in accordance with the observation of three sets of resonance signals for the alkoxido ligands in the ^1H NMR (integral ratio of 1:1:1) and $^{13}\text{C}\{^1\text{H}\}$ NMR spectra. For the $\text{Fe}(\text{CO})_4$ fragment two signals are observed in the $^{13}\text{C}\{^1\text{H}\}$ NMR spectrum, one resonance signal for the equatorial carbon atoms at δ_{eq} 216.4 ppm and one signal for the axial carbon atoms at δ_{ax} 215.8 ppm. Thus we assume that the molecular structure of compound **5** is retained after dissolution in C_6D_6 .

4. Conclusion

Starting from the bis(2-methoxyphenylmethanolate)tin(II) (**1**) and bis(2,4-dimethoxyphenylmethanolate)tin(II) (**2**), respectively, the metal carbonyl coordinated tin oxido alkoxido clusters $\{[\text{Sn}_6(\mu_3\text{-O})(\mu_3\text{-OCH}_2\text{C}_6\text{H}_4(\text{OCH}_3)_2\text{-}2,4)\{\text{W}(\text{CO})_5\}_4]\}$ (**3**), $\{[\text{Sn}_6(\mu_3\text{-O})(\mu_3\text{-OCH}_2\text{C}_6\text{H}_3(\text{OCH}_3)_2\text{-}2,4)\{\text{W}(\text{CO})_5\}_4]\}$ (**4**) and $\{[\text{Sn}_5(\mu_3\text{-O})_2(\mu\text{-OCH}_2\text{C}_6\text{H}_3(\text{OCH}_3)_2\text{-}2,4)_4(\mu_3\text{-OCH}_2\text{C}_6\text{H}_3(\text{OCH}_3)_2\text{-}2,4)\}_2\}\{\text{Fe}(\text{CO})_4\}_2$ (**5**) were synthesized in fair yield. The tin oxido clusters **3** and **4** are unprecedented representatives of a series of previously reported hexanuclear tin oxido alkoxido clusters of the general type $[\text{Sn}_6\text{O}_4(\text{OR})_4]$ ($\text{R}=\text{H, alkyl}$), which are capable to coordinate electron deficient metal complexes via lone pairs of electrons at the Sn(II) atoms. The tin atoms in these clusters build up an octahedron and in **3** and **4** the tungsten carbonyl fragments coordinate to tin atoms in the equatorial plane of an elongated octahedron. Noteworthy, the hydrolysis process to give **3** and **4** must be carefully controlled, because fully dried solvents did prevent the formation of any complex as a result of the low solubility of the tin(II) alkoxides. However larger amounts of water did produce insoluble amorphous compounds. Unexpectedly, under similar reaction conditions but in the presence of $\text{Fe}(\text{CO})_4$ ligands a pentanuclear tin oxido core of the type $[\text{Sn}_5\text{O}_2(\text{OR})_6]$ was observed to which two $\text{Fe}(\text{CO})_4$ moieties are

coordinated. This structural motif is less commonly observed for tin oxido clusters. Note, that starting from $[Sn_6(\mu_3-O)_4(\mu_3-O-SiMe_3)_4]$ Sita et al. synthesized the complexes $\{[Sn_6(\mu_3-O)_4(\mu_3-O-SiMe_3)_4]Fe(CO)_4\}_n$ ($n = 1, 2$) [17], which demonstrates that formation of the corresponding hexanuclear tin oxido benzylalcoholate complexes starting from **2** seemed to be likely as well. In conclusion, despite that a growing number of fully characterized tin oxido clusters are known, the prediction of structure formation as a result of a “controlled” hydrolysis process and thus “molecular design” of metal oxido clusters is still a great challenge.

Acknowledgements

The authors gratefully acknowledge financial support by the Deutsche Forschungsgemeinschaft (DFG), Forschergruppe 1497 “Organic-Inorganic Nanocomposites through Twin Polymerization”, BASF Aktiengesellschaft Ludwigshafen and “Eastern Europe Partnership” program (DAAD). We thank Prof. Dr. Stefan Spange, for access to measure solid state NMR, Dr. Andreas Seifert and Philipp Kitschke for measuring solid state NMR, Sebastian Saloman for water-content determination of the solvents by Karl Fischer titration and Katrin Müller for elemental analysis.

References

- [1] Q. Zhao, L. Ma, Q. Zhang, C. Wang, X. Xu, *J. Nanomater* 2015 (2015) 1–15.
- [2] J. Pan, H. Shen, S. Mathur, *J. Nanotechnol.* 2012 (2012) 1–12.
- [3] S. Das, V. Jayaraman, *Prog. Mater. Sci.* 66 (2014) 112–255.
- [4] C.G. Granqvist, A. Hultåker, *Thin Solid Films* 411 (2002) 1–5.
- [5] J.C. Yater, J.A. Yater, J.E. Yater, patent US 5889287 A, (1999).
- [6] S.S. Chadha, J.J. Alwan, patent US 5695809 A, (1997).
- [7] S.-S. Park, J.D. Mackenzie, *Thin Solid Films* 274 (1996) 154–159.
- [8] M.J. Hampden-Smith, T.A. Wark, C.J. Brinker, *Coord. Chem. Rev.* 112 (1992) 81–116.
- [9] N. Hollingsworth, G.A. Horley, M. Mazhar, M.F. Mahon, K.C. Molloy, P.W. Haycock, C.P. Myers, G.W. Critchlow, *Appl. Organomet. Chem.* 20 (2006) 687–695.
- [10] S. Mathur, V. Sivakov, H. Shen, S. Barth, C. Cavelius, A. Nilsson, P. Kuhn, *Thin Solid Films* 502 (2006) 88–93.
- [11] J.R. Brown, P.W. Haycock, L.M. Smith, A.C. Jones, E.W. Williams, *Sens. Actuators B* 63 (2000) 109–114.
- [12] R.A. Howie, W. Moser, *Nature* 219 (1968) 372–373.
- [13] P.G. Harrison, B.J. Haylett, T.J. King, *J. Chem. Soc. Chem. Commun.* (1978) 112–113.
- [14] E.V. Suslova, N.Y. Turova, V.G. Kessler, A.I. Belokon', *Russ. J. Inorg. Chem.* 52 (2007) 1682–1686.
- [15] T. Zöller, L. Iovkova-Berends, C. Dietz, T. Berends, K. Jurkschat, *Chem. Eur. J.* 17 (2011) 2361–2364.
- [16] T.J. Boyle, T.M. Alam, M.A. Rodriguez, C.A. Zechmann, *Inorg. Chem.* 41 (2002) 2574–2582.
- [17] L.R. Sita, R. Xi, G.P.A. Yap, L.M. Liable-Sands, A.L. Rheingold, *J. Am. Chem. Soc.* 119 (1997) 756–760.
- [18] I. Barbul, A.L. Johnson, G. Kociok-Köhne, K.C. Molloy, C. Silvestru, A.L. Sudlow, *ChemPlusChem* 78 (2013) 866–874.
- [19] H. Reuter, M. Kremser, *Z. Anorg. Allg. Chem.* 615 (1992) 137–142.
- [20] M. Verdenelli, S. Parola, L.G. Hubert-Pfalzgraf, S. Lecocq, *Polyhedron* 19 (2000) 2069–2075.
- [21] T. Zöller, K. Jurkschat, *Inorg. Chem.* 52 (2013) 1872–1882.
- [22] J. Caruso, M.J. Hampden-Smith, A.L. Rheingold, G. Yap, *J. Chem. Soc. Chem. Commun.* (1995) 157–158.
- [23] C. Leonhardt, S. Brumm, A. Seifert, G. Cox, A. Lange, T. Rüffer, D. Schaarschmidt, H. Lang, N. Jöhrmann, M. Hietzhold, F. Simon, M. Mehring, *ChemPlusChem* 78 (2013) 1400–1412.
- [24] F. Ribot, E. Martinez-Ferrero, K. Boubekeur, P.M.S. Hendrickx, J.C. Martins, L. Van Lokeren, R. Willem, M. Biesemans, *Inorg. Chem.* 47 (2008) 5831–5840.
- [25] B. Schiemenz, F. Ettel, G. Huttner, L. Zsolnai, *J. Organomet. Chem.* 458 (1993) 159–166.
- [26] P. Kircher, G. Huttner, L. Zsolnai, A. Driess, *Angew. Chem. Int. Ed.* 37 (1998) 1666–1668.
- [27] B. Schiemenz, B. Antelmann, G. Huttner, L. Zsolnai, *Z. Anorg. Allg. Chem.* 620 (1994) 1760–1767.
- [28] C. Wagner, K. Merzweiler, *Z. Anorg. Allg. Chem.* 628 (2002) 2241–2243.
- [29] P. Kitschke, A.A. Auer, A. Seifert, T. Rüffer, H. Lang, M. Mehring, *Inorg. Chim. Acta* 409 (Part B) (2014) 472–478.
- [30] C. Leonhardt, S. Brumm, A. Seifert, A. Lange, S. Csihony, M. Mehring, *ChemPlusChem* 79 (2014) 1440–1447.
- [31] T. Ebert, A. Seifert, S. Spange, *Macromol. Rapid Commun.* 36 (2015) 1623–1639.
- [32] A. Lange, G. Cox, K. Leitner, H. Wolf, M. Mehring, C. Leonhardt, patent US 20130069021 A1, (2013).
- [33] G. Sheldrick, *Acta Crystallogr. A* 64 (2008) 112–122.
- [34] DIAMOND-Visual Crystal Structure Information System, Crysal Impact, Postfach 1251, D-53002 Bonn, Germany, 2001.
- [35] A.V. Zubala, T. Pape, F. Hupka, A. Hepp, F.E. Hahn, *Organometallics* 28 (2009) 4221–4224.
- [36] A. Gamard, B. Jousseau, T. Toupane, G. Campet, *Inorg. Chem.* 38 (1999) 4671–4679.
- [37] D.J. Teff, C.D. Minear, D.V. Baxter, K.G. Caulton, *Inorg. Chem.* 37 (1998) 2547–2553.
- [38] T. Fjeldberg, P.B. Hitchcock, M.F. Lappert, S.J. Smith, A.J. Thorne, *J. Chem. Soc. Chem. Commun.* (1985) 939–941.
- [39] L. Wang, C.E. Kefalidis, T. Roisnel, S. Sinbandhit, L. Maron, J.-F. Carpentier, Y. Sarazin, *Organometallics* 34 (2015) 2139–2150.
- [40] L. Iovkova-Berends, T. Berends, T. Zöller, G. Bradtmöller, S. Herres-Pawlis, K. Jurkschat, *Eur. J. Inorg. Chem.* 2012 (2012) 3191–3199.
- [41] L. Iovkova-Berends, T. Berends, C. Dietz, G. Bradtmöller, D. Schollmeyer, K. Jurkschat, *Eur. J. Inorg. Chem.* 2011 (2011) 3632–3643.
- [42] R. Jambor, B. Kašná, S.G. Koller, C. Strohmann, M. Schürmann, K. Jurkschat, *Eur. J. Inorg. Chem.* 2010 (2010) 902–908.
- [43] Brian P. Johnson, S. Almstätter, F. Dielmann, M. Bodensteiner, M. Scheer, *Z. Anorg. Allg. Chem.* 636 (2010) 1275–1285.
- [44] T. Berends, L. Iovkova, G. Bradtmöller, I. Oppel, M. Schürmann, K. Jurkschat, *Z. Anorg. Allg. Chem.* 635 (2009) 369–374.
- [45] M. Veith, M. Ehses, V. Huch, *New J. Chem.* 29 (2005) 154–164.
- [46] B. Kašná, R. Jambor, M. Schürmann, K. Jurkschat, *J. Organomet. Chem.* 693 (2008) 3446–3450.
- [47] M. Henn, M. Schürmann, B. Mahieu, P. Zanello, A. Cinquantini, K. Jurkschat, *J. Organomet. Chem.* 691 (2006) 1560–1572.
- [48] M. Mantina, A.C. Chamberlin, R. Valero, C.J. Cramer, D.G. Truhlar, *J. Phys. Chem. A* 113 (2009) 5806–5812.
- [49] L. Iovkova-Berends, T. Berends, T. Zöller, D. Schollmeyer, G. Bradtmöller, K. Jurkschat, *Eur. J. Inorg. Chem.* 2012 (2012) 3463–3473.
- [50] A. Jana, R. Azhakar, H.W. Roesky, I. Objartel, D. Stalke, Z. Anorg. Allg. Chem. 637 (2011) 1795–1799.
- [51] T.J. Boyle, T.Q. Doan, L.A.M. Steele, C. Apblett, S.M. Hoppe, K. Hawthorne, R.M. Kalinich, W.M. Sigmund, *Dalton Trans.* 41 (2012) 9349–9364.